Applied and Computational Mathematics
2022; 11(3): 60-68
http://www.sciencepublishinggroup.com/j/acm
doi: 10.11648/j.acm.20221103.11
ISSN: 2328-5605 (Print); ISSN: 2328-5613 (Online)

Determination of Secondary Wavefront Aberrations in Axis-Symmetrical Optical Systems

Psang Dain Lin

Department of Mechanical Engineering, National Cheng Kung University, Tainan, Taiwan

Email address:
pdlin@mail.ncku.edu.tw

To cite this article:
Psang Dain Lin. Determination of Secondary Wavefront Aberrations in Axis-Symmetrical Optical Systems. *Applied and Computational Mathematics*. Vol. 11, No. 3, 2022, pp. 60-68. doi: 10.11648/j.acm.20221103.11

Received: April 17, 2022; **Accepted**: May 5, 2022; **Published**: May 12, 2022

Abstract: The design and development of optical systems relies on a thorough theoretical understanding of optical aberrations. However, determining the values of the various-order wavefront aberrations in an optical system is extremely challenging. Accordingly, the present study proposes a methodology for determining the numerical values of the secondary wavefront aberrations of an axis-symmetrical optical system by expanding the optical path length of its general ray using a Taylor series expansion. The determined values of the secondary wavefront aberration coefficients are given. They are distortion W511, field curvature W420, astigmatism W422, coma W331, oblique spherical aberration W240, spherical aberration W060, and six still un-named secondary wavefront aberrations. It is shown that three components (i.e., W244, W153, and W155) are not included among the secondary wavefront aberrations given in the literature despite satisfying the equations of axis-symmetrical nature of axis-symmetrical systems. In other words, the equation of existing literature fails to provide all the components needed to fully compute the secondary wavefront aberrations. By extension, some components of the higher-order wavefront aberrations may also be incompletely presented. The proposed method in this study provides the opportunity to compute all components of various-order wavefront aberrations for rotationally-symmetric optical systems, indicating it is a robust approach for aberration determination.

Keywords: Wavefront Aberrations, Geometrical Optics, Taylor Series Expansion, Optical Path Length

1. Introduction

Aberrations fall into two main classes, namely ray aberration [1] and wavefront aberration [2-5]. Wavefront aberrations describe the wavefront deformation in terms of the Optical Path Length (OPL), as measured along a general ray from the reference sphere to the wavefront. For example, Figure 1 illustrates the path of a general ray $\bar{R}_0 = \begin{bmatrix} \bar{P}_0 & \bar{\ell}_0 \end{bmatrix}^T$ originating from an object $\bar{P}_0$ with unit directional vector $\bar{\ell}_0$ and propagating through an axis-symmetrical optical system with n boundaries. The figure additionally shows a reference sphere $\bar{r}_{\text{ref}}$ centered at $\bar{P}_{n/Gaus}$ (i.e., the Gaussian image point of $\bar{P}_0$) and passing through the on-axis exit pupil point. As shown, the chief ray $\begin{bmatrix} \bar{P}_0 & \bar{\ell}_{0/chief} \end{bmatrix}^T$ of $\bar{P}_0$ is incident on the reference sphere at point $\bar{P}_{ref/chief}$. The wavefront aberration for the general ray $\bar{R}_0$ is then determined as $W(h_0, \rho, \phi) = V_{total} - V_{total/chief}$, where V_{total} is the total OPL from $\bar{P}_0$ to $\bar{P}_{ref}$, as measured along the general ray, and $V_{total/chief}$ is the OPL from $\bar{P}_0$ to $\bar{P}_{ref/chief}$, as measured along the chief ray. The total wavefront aberration of an optical system can be calculated by raytracing. However, raytracing is of limited practical use in this regard since the orders of magnitudes of V_{total} and $V_{total/chief}$ are perhaps several hundred millimeters, while the magnitude of the wavefront aberration $W(h_0, \rho, \phi)$ is just a fraction of the wavelength. Thus, the accuracy of the raytracing results may be degraded due to rounding and truncating errors. Furthermore, it is impossible to decompose the values of $W(h_0, \rho, \phi)$ obtained from raytracing into their constituent orders and components.

Many approaches for exploring the aberrations of axis-symmetrical systems have been proposed [1–17]. One

such method (Eqs. (3.31a) and (3.31b) of [3]) exploits the axis-symmetrical natural of axis-symmetrical systems to express $W(h_0,\rho,\phi)$ as:

$$W(h_0,\rho,\phi)=\sum_{j=0}^{\infty}\sum_{p=0}^{\infty}\sum_{m=0}^{\infty}C_{(2j+m)(2p+m)m}(h_0)^{2j+m}(\rho)^{2p+m}(C\phi)^m, \quad (1)$$

where j, p and m are non-negative integers, ρ and ϕ are the polar coordinates of the entrance pupil (Figure 2), h_0 is the object height, and $C\phi$ denotes $\cos\phi$. From Eq. (1) the following wavefront aberrations are listed up to the sixth order in Tables on pages 157 and 158 of [3]:

$$W=\Delta W_{0th}+\Delta W_{2nd}+\Delta W_{4th}+\Delta W_{6th}, \quad (2)$$

where ΔW_{0th}, ΔW_{2nd}, ΔW_{4th} and ΔW_{6th} are the zeroth-, second-, fourth-, and sixth-order aberrations, respectively, and are given by

$$\Delta W_{0th}=C_{000} \quad (3)$$

$$\Delta W_{2nd}=C_{020}\rho^2+C_{111}h_0\rho C\phi+C_{200}h_0^2 \quad (4)$$

$$\Delta W_{4th}=C_{040}\rho^4+C_{131}h_0\rho^3C\phi+C_{222}h_0^2\rho^2C^2\phi+C_{220}h_0^2\rho^2+C_{311}h_0^3\rho C\phi+C_{400}h_0^4 \quad (5)$$

$$\begin{aligned}\Delta W_{6th}=&C_{060}\rho^6+C_{151}h_0\rho^5C\phi+C_{242}h_0^2\rho^4C^2\phi+C_{333}h_0^3\rho^3C^3\phi+C_{240}h_0^2\rho^4+C_{331}h_0^3\rho^3C\phi\\&+C_{422}h_0^4\rho^2C^2\phi+C_{420}h_0^4\rho^2+C_{511}h_0^5\rho C\phi+C_{600}h_0^6\end{aligned} \quad (6)$$

It is noted that Eq. (1) can not only decompose the wavefront aberration into different orders, but can also decompose each order aberration into different components. For example, components $C_{040}\rho^4$, $C_{131}h_0\rho^3C\phi$, $C_{222}h_0^2\rho^2C^2\phi$, $C_{220}h_0^2\rho^2$, $C_{311}h_0^3\rho C\phi$ and $C_{400}h_0^4$ in ΔW_{4th} are the spherical, coma, astigmatism, field curvature, distortion and quartic piston aberrations, respectively. Notably, Eq. (1) can provide the components of the primary wavefront aberrations. However, as shown later in this study, components $C_{244}h_0^2\rho^4C^4\phi$, $C_{153}h_0\rho^5C^3\phi$, and $C_{155}h_0\rho^5C^5\phi$, which satisfy the equations derived from the axis-symmetrical property of axial-symmetric systems, are missing in ΔW_{6th}. In other words, Eq. (1) fails to provide all the components needed to fully compute the secondary aberrations. By extension, it is reasonable to assume that Eq. (1) may also fail to provide some components of the tertiary and higher-order wavefront aberrations.

Although Eq. (1) can decompose the wavefront aberration into various orders and components, it cannot determine the values of the leading C coefficients. Many approaches for determining these coefficients have been proposed [1–17]. One of the most commonly used methods is that developed by Buchdahl [6], in which the marginal and principal paraxial rays are traced, and the results are then used to compute the unconverted third-order Buchdahl aberration coefficients (denoted as $\sigma_j, j=1-5$). These sigma coefficients are then converted into transverse, longitudinal and wave aberration coefficients as required. Many commercial optical design and analysis programs use Buchdahl's approach to determine the primary wavefront and ray aberrations (e.g., Zemax [18]). However, Zemax still fails to provide the numerical values of the secondary wavefront aberrations, since its formulae is relatively complicated.

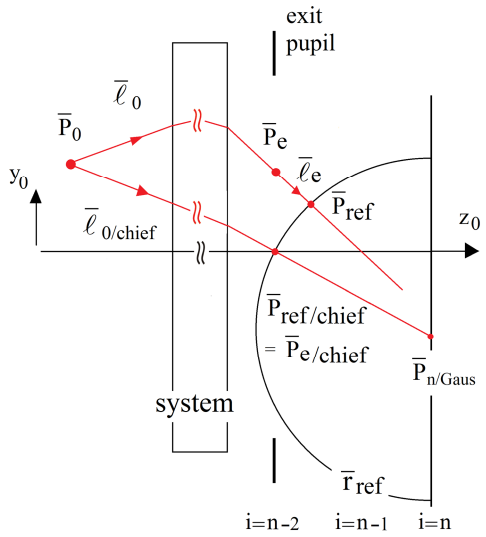

Figure 1. *Reference sphere* $\bar{r}_{ref}$ *centered at Gaussian imaging point* $\bar{P}_{n/Gaus}$.

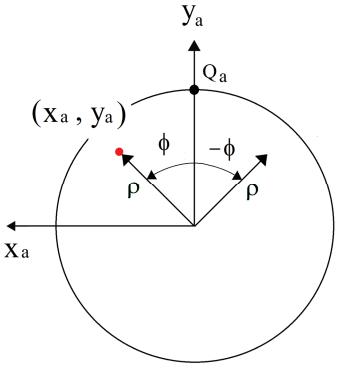

Figure 2. *Entrance pupil with in-plane Cartesian coordinates* (x_a, y_a) *and polar coordinates* (ρ,ϕ).

As noted in the beginning, the total wavefront aberration of an optical system can be calculated by tracing skew rays. However, skewray equations are recursive functions and are not convenient for many applications. The most elegant solution in mathematics for this type of hard problem is the Taylor series expansion to convert the functions into polynomial equations (e.g., [19, 20]). It is also shown that obtained polynomial ray equations can provide an effective means of determining an appropriate search during the system design process (e.g., [21]). Accordingly, the present study proposes a method for determining the values of the C coefficients for the secondary wavefront aberrations of an axis-symmetrical optical system based on the Taylor series expansion of the OPL of a skew ray.

2. Taylor Series Expansion of Opl

When analyzing an axis-symmetrical optical system containing n boundaries, the first step is to label the boundaries sequentially from i=0 to i=n (e.g., Figure 3 with the parameters listed in Table 1). As illustrated in Figure 4, in a medium of constant refractive index ξ_{i-1}, the OPL between points $\bar{P}_{i-1}$ and $\bar{P}_i$ (denoted as V_i) of a general ray is given by the product of ξ_{i-1} and the geometric length λ_i between them. That is,

$$V_i = \xi_{i-1}\lambda_i . \tag{7}$$

As described in [17], V_i can be approximated by its Taylor series expansion up to the sixth-order as follows:

$$V_i(\bar{Y}_0) \approx V_{i/0th}(\bar{Y}_{0/axis}) + \Delta V_{i/1st} + \Delta V_{i/2nd} + \Delta V_{i/3rd} + \Delta V_{i/4th} + \Delta V_{i/5th} + \Delta V_{i/6th} \tag{8}$$

where $\bar{Y}_{0/axis}$ is the ray originating from the on-axis point $\bar{P}_{0/axis} = \begin{bmatrix} 0 & 0 & P_{0z} \end{bmatrix}^T$ with unit directional vector $\bar{\ell}_{0/axis} = \begin{bmatrix} 0 & 0 & 1 \end{bmatrix}^T$, and is defined as (Eq. (7) of [17]):

$$\bar{Y}_{0/axis} = \begin{bmatrix} 0 & 0 & P_{0z} & 0 & 0 \end{bmatrix}^T . \tag{9}$$

The zeroth-order term (i.e., $V_{i/0th}(\bar{Y}_{0/axis})$ is a constant value for any ray originating from $\bar{P}_0 = \begin{bmatrix} 0 & h_0 & P_{0z} \end{bmatrix}^T$. Furthermore, for axis-symmetrical systems, the first-, third-, and fifth-order expansions vanish as a consequence of the rotational symmetry of the system. Among the remaining expansions, the second-order expansion $\Delta V_{i/2nd}$ provides the magnification and defocus coefficients, while the fourth-order expansion $\Delta V_{i/4th}$ is responsible for the primary wavefront aberrations [17]. To investigate the secondary wavefront aberrations, one has to start from the following sixth-order expansion of V_i (i=1 to i=n-1) with respect to the independent variables h_0, y_a and $(y_a - h_0)$:

$$\begin{aligned}
\Delta V_{i/6th} = \frac{1}{720}\Bigg(& \frac{\partial^6 V_i}{\partial h_0^6}h_0^6 + 6\frac{\partial^6 V_i}{\partial h_0^5 \partial x_a}h_0^5 x_a + 6\frac{\partial^6 V_i}{\partial h_0^5 \partial (y_a - h_0)}h_0^5 (y_a - h_0) + 15\frac{\partial^6 V_i}{\partial h_0^4 \partial x_a^2}h_0^4 x_a^2 + 30\frac{\partial^6 V_i}{\partial h_0^4 \partial x_a \partial (y_a - h_0)}h_0^4 x_a (y_a - h_0) \\
& + 15\frac{\partial^6 V_i}{\partial h_0^4 \partial (y_a - h_0)^2}h_0^4 (y_a - h_0)^2 + 20\frac{\partial^6 V_i}{\partial h_0^3 \partial x_a^3}h_0^3 x_a^3 + 60\frac{\partial^6 V_i}{\partial h_0^3 \partial x_a^2 \partial (y_a - h_0)}h_0^3 x_a^2 (y_a - h_0) + 60\frac{\partial^6 V_i}{\partial h_0^3 \partial x_a \partial (y_a - h_0)^2}h_0^3 x_a (y_a - h_0)^2 \\
& + 20\frac{\partial^6 V_i}{\partial h_0^3 \partial (y_a - h_0)^3}h_0^3 (y_a - h_0)^3 + 15\frac{\partial^6 V_i}{\partial h_0^2 \partial x_a^4}h_0^2 x_a^4 + 60\frac{\partial^6 V_i}{\partial h_0^2 \partial x_a^3 \partial (y_a - h_0)}h_0^2 x_a^3 (y_a - h_0) + 90\frac{\partial^6 V_i}{\partial h_0^2 \partial x_a^2 \partial (y_a - h_0)^2}h_0^2 x_a^2 (y_a - h_0)^2 \\
& + 60\frac{\partial^6 V_i}{\partial h_0^2 \partial x_a \partial (y_a - h_0)^3}h_0^2 x_a (y_a - h_0)^3 + 15\frac{\partial^6 V_i}{\partial h_0^2 \partial (y_a - h_0)^4}h_0^2 (y_a - h_0)^4 + 6\frac{\partial^6 V_i}{\partial h_0 \partial x_a^5}h_0 x_a^5 + 30\frac{\partial^6 V_i}{\partial h_0 \partial x_a^4 \partial (y_a - h_0)}h_0 x_a^4 (y_a - h_0) \\
& + 60\frac{\partial^6 V_i}{\partial h_0 \partial x_a^3 \partial (y_a - h_0)^2}h_0 x_a^3 (y_a - h_0)^2 + 60\frac{\partial^6 V_i}{\partial h_0 \partial x_a^2 \partial (y_a - h_0)^3}h_0 x_a^2 (y_a - h_0)^3 + 30\frac{\partial^6 V_i}{\partial h_0 \partial x_a \partial (y_a - h_0)^4}h_0 x_a (y_a - h_0)^4 \\
& + 6\frac{\partial^6 V_i}{\partial h_0 \partial (y_a - h_0)^5}h_0 (y_a - h_0)^5 + \frac{\partial^6 V_i}{\partial x_a^6}x_a^6 + 6\frac{\partial^6 V_i}{\partial x_a^5 \partial (y_a - h_0)}x_a^5 (y_a - h_0) + 15\frac{\partial^6 V_i}{\partial x_a^4 \partial (y_a - h_0)^2}x_a^4 (y_a - h_0)^2 \\
& + 20\frac{\partial^6 V_i}{\partial x_a^3 \partial (y_a - h_0)^3}x_a^3 (y_a - h_0)^3 + 15\frac{\partial^6 V_i}{\partial x_a^2 \partial (y_a - h_0)^4}x_a^2 (y_a - h_0)^4 + 6\frac{\partial^6 V_i}{\partial x_a \partial (y_a - h_0)^5}x_a (y_a - h_0)^5 + \frac{\partial^6 V_i}{\partial (y_a - h_0)^6}(y_a - h_0)^6 \Bigg).
\end{aligned} \tag{10}$$

When determining wavefront aberrations, the leading coefficients of $\partial^{f+g+h} V_i / \partial h_0^f \partial x_a^g \partial (y_a - h_0)^h$ in Eq. (10) must be evaluated at the chosen ray $\bar{Y}_{0/axis}$. After combining the expanded terms of Eq. (10), the following expression is obtained for $\Delta V_{i/6th}$ in terms of h_0, x_a and y_a:

$$\begin{aligned}\Delta V_{i/6th} = & g_{i/600}h_0^6 + g_{i/510}h_0^5 x_a + g_{i/501}h_0^5 y_a + g_{i/420}h_0^4 x_a^2 + g_{i/411}h_0^4 x_a y_a + g_{i/402}h_0^4 y_a^2 + g_{i/330}h_0^3 x_a^3 + g_{i/321}h_0^3 x_a^2 y_a \\ & + g_{i/312}h_0^3 x_a y_a^2 + g_{i/303}h_0^3 y_a^3 + g_{i/240}h_0^2 x_a^4 + g_{i/231}h_0^2 x_a^3 y_a + g_{i/222}h_0^2 x_a^2 y_a^2 + g_{i/213}h_0^2 x_a y_a^3 + g_{i/204}h_0^2 y_a^4 + g_{i/150}h_0 x_a^5 \\ & + g_{i/141}h_0 x_a^4 y_a + g_{i/132}h_0 x_a^3 y_a^2 + g_{i/123}h_0 x_a^2 y_a^3 + g_{i/114}h_0 x_a y_a^4 + g_{i/105}h_0 y_a^5 + g_{i/060}x_a^6 + g_{i/051}x_a^5 y_a + g_{i/042}x_a^4 y_a^2 \\ & + g_{i/033}x_a^3 y_a^3 + g_{i/024}x_a^2 y_a^4 + g_{i/015}x_a y_a^5 + g_{i/006}y_a^6,\end{aligned} \tag{11}$$

The first, second and third post-subscripts of the g coefficients in Eq. (11) refer to the powers of h_0, x_a and y_a, respectively. The present study uses numerically-determined derivatives (i.e., $\partial^{f+g+h}V_i / \partial h_0^f \partial x_a^g \partial (y_a - h_0)^h$) to compute the g coefficients. It is found that the following g coefficients are all equal to zero:

$$g_{i/510} = g_{i/411} = g_{i/330} = g_{i/312} = g_{i/231} = g_{i/213} = g_{i/150} = g_{i/132} = g_{i/114} = g_{i/033} = g_{i/015} = g_{i/051} = 0.$$

Thus, the sixth-order expansion of V_i (i=1 to i=n-1) in Eq. (11) can be simplified as

$$\begin{aligned}\Delta V_{i/6th} = & g_{i/600}h_0^6 + g_{i/501}h_0^5 y_a + g_{i/420}h_0^4 x_a^2 + g_{i/402}h_0^4 y_a^2 + g_{i/321}h_0^3 x_a^2 y_a + g_{i/303}h_0^3 y_a^3 + g_{i/240}h_0^2 x_a^4 + g_{i/222}h_0^2 x_a^2 y_a^2 \\ & + g_{i/204}h_0^2 y_a^4 + g_{i/141}h_0 x_a^4 y_a + g_{i/123}h_0 x_a^2 y_a^3 + g_{i/105}h_0 y_a^5 + g_{i/042}x_a^4 y_a^2 + g_{i/024}x_a^2 y_a^4 + g_{i/060}x_a^6 + g_{i/006}y_a^6,\end{aligned} \tag{12}$$

where the expressions of the g coefficients are listed in Appendix. The values of g coefficients can be determined by coding these equations using the FORTRAN program. The term $g_{i/600}$ is referred to as the piston term since this term do not involve x_a or y_a. Furthermore, since all the g coefficients are evaluated at $\bar{Y}_{0/axis}$ (i.e., a ray travelling along the optica axis), and Eqs. (38) and (39) of Appendix do not involve partial derivatives with respect to ∂h_0, it follows that the numerical values of $g_{i/042}$ and $g_{i/024}$ are equal. That is,

$$g_{i/042} = g_{i/024} \tag{13}$$

Similarly, the numerical values of $g_{i/060}$ and $g_{i/006}$ are also equal, i.e.,

$$g_{i/060} = g_{i/006} \tag{14}$$

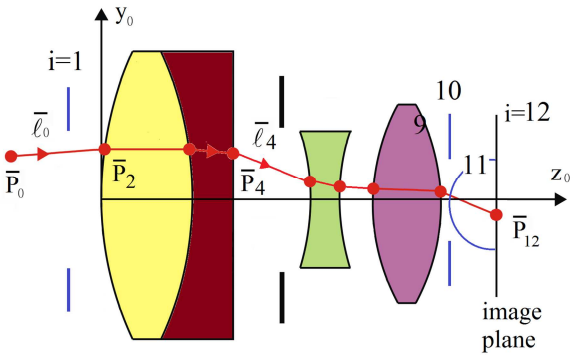

Figure 3. *Petzval lens system with n=12 boundaries.*

Table 1. *Specification of illustrative axis-symmetrical system shown in Figure 3.*

Boundary i	radius	separation	refractive index
0 (object)		222.103275	1.00000
1 (entrance pupil)	0	-22.103275	1.00000
2	38.22190	15.84960	1.65000
3	-56.08570	5.96900	1.71736
4	-590.68200	3.02260	1.00000
5 (aperture)	0	14.02080	1.00000
6	-41.79570	2.514600	1.52583
7	29.34460	7.924800	1.00000
8	63.56350	6.09600	1.65000
9	-56.86550	-39.110352	1.00000
10 (exit pupil)	0	0	1.00000
11 (reference sphere)	R_{ref}	131.198822	1.00000
12 (image surface)	0		

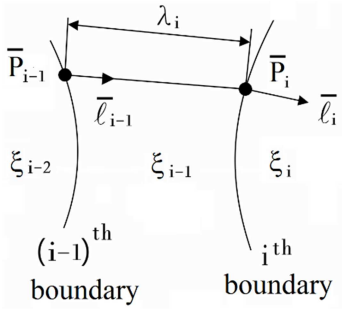

Figure 4. *Optical path length* V_i *is given by product of geometric length* λ_i *between points* $\bar{P}_{i-1}$ *and* $\bar{P}_i$ *and refractive index* ξ_{i-1} *of intermediate medium.*

3. Expressions of C Coefficients

Let V_{total} denote the OPL measured along the general ray $\bar{R}_0 = \begin{bmatrix} \bar{P}_0 & \bar{\ell}_0 \end{bmatrix}^T$ from object $\bar{P}_0$ to the incidence point on the reference sphere $\bar{P}_{ref}$. V_{total} can be determined by summing all the OPLs from object $\bar{P}_0$ to $\bar{P}_{ref}$, i.e.,

$$V_{total} = V_1 + V_2 + \ldots + V_i + \ldots + V_{n-2} + V_{n-1} = \sum_{i=1}^{n-1} V_i. \tag{15}$$

From Eqs. (8) and (15), the sixth-order Taylor series expansion of V_{total}, denoted as $\Delta V_{total/6th}$, can be obtained simply as

$$\Delta V_{total/6th} = \sum_{i=1}^{n-1} \Delta V_{i/6th} , \tag{16}$$

where $\Delta V_{i/6th}$ (i=1 to i=n-1) is given already in Eq. (12).

As noted previously, Figure 1 shows the chief ray of object $\bar{P}_0$ and its incidence point $\bar{P}_{ref/chief}$ on the reference sphere. The chief ray is in fact a particular ray originating from $\bar{P}_0$ and passing through the center of aperture of the system (i.e., $(x_a, y_a) = (0,0)$). Thus, the sixth-order Taylor series expansion of the OPL of the chief ray, denoted as $\Delta V_{total/chief/6th}$, can be determined from Eq. (12) by setting $(x_a, y_a) = (0,0)$, to give

$$\Delta V_{total/chief/6th} = \sum_{i=1}^{n-1} g_{i/600} h_0^6 . \tag{17}$$

The difference between Eqs. (16) and (17) (i.e., $V_{total/6th} - \Delta V_{total/chief/6th}$) then gives the secondary wavefront aberration ΔW_{6th} of the general ray $\bar{R}_0$ as

$$\begin{aligned}
\Delta W_{6th} = \sum_{i=1}^{n-1} \Big[& g_{i/501} h_0^5 y_a + (g_{i/420} - g_{i/402}) h_0^4 x_a^2 + g_{i/402} h_0^4 (x_a^2 + y_a^2) + g_{i/321} h_0^3 x_a^2 y_a + g_{i/303} h_0^3 y_a^3 \\
& + (g_{i/240} - g_{i/204}) h_0^2 x_a^4 + (g_{i/222} - 2g_{i/204}) h_0^2 x_a^2 y_a^2 + g_{i/204} h_0^2 (x_a^2 + y_a^2)^2 + g_{i/123} h_0 x_a^2 y_a^3 \\
& + g_{i/141} h_0 x_a^4 y_a + g_{i/105} h_0 y_a^5 + (g_{i/060} - g_{i/006}) x_a^6 + (g_{i/042} - g_{i/024} - 3g_{i/006}) x_a^4 y_a^2 \\
& + g_{i/006} (x_a^2 + y_a^2)^3 - 3g_{i/006} x_a^2 y_a^4 + g_{i/024} x_a^2 y_a^2 (x_a^2 + y_a^2) \Big] \\
= \sum_{i=1}^{n-1} \Big[& g_{i/501} h_0^5 \rho C\phi + g_{i/420} h_0^4 \rho^2 + (g_{i/402} - g_{i/420}) h_0^4 \rho^2 C^2\phi + g_{i/321} h_0^3 \rho^3 C\phi + (g_{i/303} - g_{i/321}) h_0^3 \rho^3 C^3\phi \\
& + g_{i/240} h_0^2 \rho^4 + (g_{i/222} - 2g_{i/240}) h_0^2 \rho^4 C^2\phi + (g_{i/204} - g_{i/222} + g_{i/240}) h_0^2 \rho^4 C^4\phi \\
& + g_{i/141} h_0 \rho^5 C\phi + (g_{i/123} - 2g_{i/141}) h_0 \rho^5 C^3\phi + (g_{i/141} - g_{i/123} + g_{i/105}) h_0 \rho^5 C^5\phi \\
& + g_{i/060} \rho^6 + (g_{i/042} - 3g_{i/060}) \rho^6 C^2\phi + (g_{i/024} - 2g_{i/042} + 3g_{i/060}) \rho^6 C^4\phi \\
& + (g_{i/006} - g_{i/060} + g_{i/042} - g_{i/024}) \rho^6 C^6\phi \Big] \\
= & C_{511} h_0^5 \rho C\phi + C_{420} h_0^4 \rho^2 + C_{422} h_0^4 \rho^2 C^2\phi + C_{331} h_0^3 \rho^3 C\phi + C_{333} h_0^3 \rho^3 C^3\phi \\
& + C_{240} h_0^2 \rho^4 + C_{242} h_0^2 \rho^4 C^2\phi + C_{244} h_0^2 \rho^4 C^4\phi + C_{151} h_0 \rho^5 C\phi + C_{153} h_0 \rho^5 C^3\phi \\
& + C_{155} h_0 \rho^5 C^5\phi + C_{060} \rho^6 + C_{062} \rho^6 C^2\phi + C_{064} \rho^6 C^4\phi + C_{066} \rho^6 C^6\phi .
\end{aligned} \tag{18}$$

One has to note that both $(x_a, y_a) = (\rho S\phi, \rho C\phi)$ and $S^2\phi = 1 - C^2\phi$ are used in Eq. (18). It is also noted that the first, second and third post-subscripts of the C coefficients in Eq. (18) represent the powers of h_0, ρ and $C\phi$, respectively. The sum of the first two post-subscripts of C_{511}, for example, indicates that C_{511} is one C coefficient of the sixth-order expansion. The C coefficients of Eq. (18) are defined as follows:

$$C_{511} = \sum_{i=1}^{n-1} g_{i/501} , \; C_{420} = \sum_{i=1}^{n-1} g_{i/420} , \; C_{422} = \sum_{i=1}^{n-1} (g_{i/402} - g_{i/420}) , \; C_{331} = \sum_{i=1}^{n-1} g_{i/321} , \; C_{240} = \sum_{i=1}^{n-1} g_{i/240} , \; C_{060} = \sum_{i=1}^{n-1} g_{i/060} ,$$

$$C_{151} = \sum_{i=1}^{n-1} g_{i/141} , \; C_{242} = \sum_{i=1}^{n-1} (g_{i/222} - 2g_{i/240}) , \; C_{333} = \sum_{i=1}^{n-1} (g_{i/303} - g_{i/321}) , \; C_{244} = \sum_{i=1}^{n-1} (g_{i/204} - g_{i/222} + g_{i/240}) ,$$

$$C_{153} = \sum_{i=1}^{n-1} (g_{i/123} - 2g_{i/141}) , \; C_{155} = \sum_{i=1}^{n-1} (g_{i/141} - g_{i/123} + g_{i/105}) , \; C_{062} = \sum_{i=1}^{n-1} (g_{i/042} - 3g_{i/060}) ,$$

$$C_{064} = \sum_{i=1}^{n-1} (g_{i/024} - 2g_{i/042} + 3g_{i/060}) = -C_{062} , \; C_{066} = \sum_{i=1}^{n-1} (g_{i/006} - g_{i/060} + g_{i/042} - g_{i/024}) = 0 . \tag{19}$$

Equations (13) and (14) are used to simplify C_{064} and C_{066} of Eq. (19).

4. Secondary Wavefront Aberrations

Equation (19) enable the determination of the C coefficients for a general ray. In the discussions which follow, the object in Figure 3 is assumed to be positioned at $P_{0z} = -200$, the image plane is the Gaussian image plane (i.e., the separation distance of the image plane i=12 from surface i=9 is 92.088474), where all lengths have units of mm). In addition, the radius of the entrance pupil is $\rho_{\max} = 21$. The methodology proposed in this study was implemented in self-written FORTRAN code. From Eq. (19), the values of the C coefficients are obtained as:

$$C_{511}= 0.03430\times10^{-10},\ C_{420}=0.03720\times10^{-10},\ C_{422}= 0.00353\times10^{-10},\ C_{331}= -0.23403\times10^{-10},\ C_{240}=0.26685\times10^{-10},$$
$$C_{060} = -0.10079\times10^{-10},\ C_{151}=-0.62709\times10^{-10},\ C_{242}= 0.62732\times10^{-10},\ C_{333}=-0.15466\times10^{-10},\ C_{244}= 0.01924\times10^{-10},$$
$$C_{153}= 0.12480\times10^{-10},\ C_{155}=-0.00693\times10^{-10},\ C_{062}+C_{064}=0,\ C_{066}=0.$$

It is noted that different researchers may use different terminologies to describe wavefront aberrations. For example, it is possible to utilize C_{060}, C_{331}, C_{422}, C_{420} and C_{511} to refer to secondary spherical aberration, coma, astigmatism, field curvature and distortion, respectively. The present study follows the notation conventions of Zemax [18] and Johanson [4] by using the aberrations of the ray passing through point Q_a on the entrance pupil (i.e., the maximum entrance pupil radius $\rho = \rho_{\max}$ with $C\phi = 1$, see Figure 2) to represent the secondary wavefront aberrations. The aberrations for any ray with other values of ρ and ϕ can be determined simply using appropriate scaling factors (i.e., $\rho/\rho_{\max}$ and $C\phi$). The wavefront aberrations are often divided by the wavelength $\upsilon_0 = 0.00055$. In other words, the secondary aberrations can be described as

$$Wjpm = C_{jpm}(h_0)^j(\rho_{\max})^p(C0^o)^m/\upsilon_0 = C_{jpm}(h_0)^j(\rho_{\max})^p/\upsilon_0. \quad (20)$$

The aberration $C_{153}h_0\rho^5C^3\phi$ of the ray passing (ρ,ϕ), for example, can be determined from $W153$ by $W153(\rho/\rho_{\max})^5(C\phi)^3\upsilon_0$. Based on the C coefficients given above and Eq. (20), the distortion W511, field curvature W420, astigmatism W422, coma W331, oblique spherical aberration W240, and spherical aberration W060 can be computed from the proposed method as

$$W511 = C_{511}h_0^5\rho_{\max}/\upsilon_0 = 0.185925,\ W420 = C_{420}h_0^4\rho_{\max}^2/\upsilon_0 = 0.249131,\ W422 = C_{422}h_0^4\rho_{\max}^2/\upsilon_0 = 0.023644,$$
$$W331 = C_{331}h_0^3\rho_{\max}^3/\upsilon_0 = -1.936011,\ W240 = C_{240}h_0^2\rho_{\max}^2/\upsilon_0 = 2.726958,\ W060 = C_{060}\rho_{\max}^6/\upsilon_0 = -1.571733. \quad (21)$$

The following are six still un-named secondary aberrations when $W062 + W064 = 0$ and $W066 = C_{066}\rho_{\max}^6/\upsilon_0 = 0$ are ignored:

$$W151 = C_{151}h_0\rho_{\max}^5/\upsilon_0 = -7.916136,\ W242 = C_{242}h_0^2\rho_{\max}^4/\upsilon_0 = 6.410636,\ W333 = C_{333}h_0^3\rho_{\max}^3/\upsilon_0 = -1.279410,$$
$$W244 = C_{244}h_0^2\rho_{\max}^4/\upsilon_0 = 0.196324,\ W153 = C_{153}h_0\rho_{\max}^5/\upsilon_0 = 1.575386,\ W155 = C_{155}h_0\rho_{\max}^5/\upsilon_0 = -0.087512. \quad (22)$$

As stated in the Introduction, Zemax does not provide the values of the secondary wavefront aberrations. Therefore, it is necessary to use the fifth-order derivatives of the OPL to validate the proposed methodology. From Table 2, it is seen that the numerical results obtained from the two methods are in good agreement. Furthermore, the value of the total wavefront aberration determined from raytracing, i.e., $W(h_0,\rho,\phi) = -131.895732\upsilon_0$, is also in reasonable agreement with the sum of the primary and secondary wavefront aberrations (i.e., $\Delta W_{4th} + \Delta W_{6th} = -133.281438\upsilon_0 - 1.422798\upsilon_0 = -134.704236\upsilon_0$) from the proposed method. The difference between them ($-2.808498\upsilon_0$) is attributed to higher-order aberrations.

As also stated in the Introduction, it is impossible to have components $C_{244}h_0^2\rho^4C^4\phi$, $C_{153}h_0\rho^5C^3\phi$, and $C_{155}h_0\rho^5C^5\phi$ from Eq. (1) when j, p and m are confined to non-negative integers. Equation (1) derives from the fact that the aberration function $W(h_0,\rho,\phi)$ must satisfy the following equations based on the axis-symmetrical nature of axis-symmetrical systems (P. 154 of [2]):

$$W(0,\rho,\phi) = W(0,-\rho,\phi) \quad (23)$$

$$W(h_0,\rho,\phi) = W(h_0,\rho,-\phi) \quad (24)$$

$$W(h_0,\rho,\phi) = W(-h_0,\rho,\pi+\phi) = W(-h_0,\rho,\pi-\phi) \quad (25)$$

Equation (23) implies that the components of $W(h_0,\rho,\phi)$ that do not depend on h_0 should vary as ρ^2, or as its integer power. Meanwhile, Eq. (24) indicates that $W(h_0,\rho,\phi)$ must be a function of $C\phi$. Finally, Eq. (25) shows that $W(h_0,\rho,\phi)$ corresponding to an object with height h_0 above the optical

axis must equal $W(-h_0,\rho,\pi+\phi)$, and $W(-h_0,\rho,\pi-\phi)$ for an object with a height h_0 below the optical axis. It should be noted that the missing components (i.e., $C_{244}h_0^2\rho^4C^4\phi$, $C_{153}h_0\rho^5C^3\phi$, and $C_{155}h_0\rho^5C^5\phi$) satisfy Eqs. (23)-(25). Consequently, Eq. (1) is only a sufficient condition, not a necessary and sufficient condition, for the axis-symmetrical nature of axis-symmetrical systems. If j, p and m of Eq. (1) are not confined to non-negative integer values, the missing components $C_{244}h_0^2\rho^4C^4\phi$, $C_{153}h_0\rho^5C^3\phi$, and $C_{155}h_0\rho^5C^5\phi$ can be obtained from (j,p,m)= (-1,0,4), (-1,1,3), and (-2,0,5), respectively.

Table 2. *Numerical values of secondary wavefront Wjpm coefficients obtained using fifth-order derivatives of OPL. Their percentage errors compared with the proposed method are less than 0.001%.*

W511= 0.185926	W420= 0.249130	W422= 0.023640
W331= -1.936007	W240= 2.726957	W060= -1.571733
W151= -7.916133	W242= 6.410633	W333= -1.279406
W244= 0.196322	W153= -1.575385	W155= -0.087511

5. Conclusions

The wavefront aberration of an optical system is defined as the optical path difference between a general ray V_{total} and the chief ray $V_{total/chief}$ measured from the object to the reference sphere. It is impossible to decompose $W(h_0,\rho,\phi)$ into its various-order aberrations and components by raytracing. Accordingly, this study has proposed a method for decomposing the secondary wavefront aberrations of an axis-symmetrical optical system by expanding the OPL of the general ray as a Taylor series expansion. The sixth-order wavefront aberrations ΔW_{6th} of the system have then been obtained by computing the OPL difference $V_{total/6th}-V_{total/chief/6th}$. Notably, the proposed method uses numerically-determined derivatives to generate the information needed to compute the wavefront aberration coefficients, and thus the equations based on the axis-symmetrical nature of axis-symmetrical systems are not required. It has been shown that the wavefront aberration function provided in the literature (e.g., [3]) is a sufficient condition only, not a necessary and sufficient condition, for the axis-symmetrical nature of axis-symmetrical systems. Consequently, three components of the secondary wavefront aberrations are missing. As a result, some components of the higher-order aberrations may also be incompletely presented. By contrast, the method proposed in this study provides the opportunity to compute the higher-order aberration coefficients simply by generating higher-order partial derivative matrices. It is anticipated that the proposed method can thus provide a more accurate evaluation of the system aberrations in rotationally-symmetric optical systems.

Funding

Ministry of Science and Technology, Taiwan (MOST) (110-2221-E-006-178).

Acknowledgements

The support, motivation and encouragement offered by my colleague, Professor R. Barry Johnson (Alabama Agricultural & Mechanical University) throughout the study of ray aberrations is greatly appreciated.

Appendix

$$g_{i/600}=\frac{1}{720}\left(\frac{\partial^6V_i}{\partial h_0^6}+\frac{\partial^6V_i}{\partial(y_a-h_0)^6}-6\frac{\partial^6V_i}{\partial h_0^5\partial(y_a-h_0)}-6\frac{\partial^6V_i}{\partial h_0\partial(y_a-h_0)^5}+15\frac{\partial^6V_i}{\partial h_0^4\partial(y_a-h_0)^2}+15\frac{\partial^6V_i}{\partial h_0^2\partial(y_a-h_0)^4}-20\frac{\partial^6V_i}{\partial h_0^3\partial(y_a-h_0)^3}\right) \quad (26)$$

$$g_{i/501}=\frac{1}{120}\left(-\frac{\partial^6V_i}{\partial(y_a-h_0)^6}+\frac{\partial^6V_i}{\partial h_0^5\partial(y_a-h_0)}+5\frac{\partial^6V_i}{\partial h_0\partial(y_a-h_0)^5}-5\frac{\partial^6V_i}{\partial h_0^4\partial(y_a-h_0)^2}-10\frac{\partial^6V_i}{\partial h_0^2\partial(y_a-h_0)^4}+10\frac{\partial^6V_i}{\partial h_0^3\partial(y_a-h_0)^3}\right) \quad (27)$$

$$g_{i/420}=\frac{1}{48}\left(\frac{\partial^6V_i}{\partial h_0^4\partial x_a^2}+\frac{\partial^6V_i}{\partial x_a^2\partial(y_a-h_0)^4}-4\frac{\partial^6V_i}{\partial h_0^3\partial x_a^2\partial(y_a-h_0)}-4\frac{\partial^6V_i}{\partial h_0\partial x_a^2\partial(y_a-h_0)^3}+6\frac{\partial^6V_i}{\partial h_0^2\partial x_a^2\partial(y_a-h_0)^2}\right) \quad (28)$$

$$g_{i/402}=\frac{1}{48}\left(\frac{\partial^6V_i}{\partial(y_a-h_0)^6}-4\frac{\partial^6V_i}{\partial h_0\partial(y_a-h_0)^5}+\frac{\partial^6V_i}{\partial h_0^4\partial(y_a-h_0)^2}+6\frac{\partial^6V_i}{\partial h_0^2\partial(y_a-h_0)^4}-4\frac{\partial^6V_i}{\partial h_0^3\partial(y_a-h_0)^3}\right) \quad (29)$$

$$g_{i/321}=\frac{1}{12}\left(-\frac{\partial^6V_i}{\partial x_a^2\partial(y_a-h_0)^4}+\frac{\partial^6V_i}{\partial h_0^3\partial x_a^2\partial(y_a-h_0)}+3\frac{\partial^6V_i}{\partial h_0\partial x_a^2\partial(y_a-h_0)^3}-3\frac{\partial^6V_i}{\partial h_0^2\partial x_a^2\partial(y_a-h_0)^2}\right) \quad (30)$$

$$g_{i/303}=\frac{1}{36}\left(-\frac{\partial^6V_i}{\partial(y_a-h_0)^6}+3\frac{\partial^6V_i}{\partial h_0\partial(y_a-h_0)^5}-3\frac{\partial^6V_i}{\partial h_0^2\partial(y_a-h_0)^4}+\frac{\partial^6V_i}{\partial h_0^3\partial(y_a-h_0)^3}\right) \quad (31)$$

$$g_{i/240} = \frac{1}{48}\left(\frac{\partial^6 V_i}{\partial h_0^2 \partial x_a^4} + \frac{\partial^6 V_i}{\partial x_a^4 \partial (y_a - h_0)^2} - 2\frac{\partial^6 V_i}{\partial h_0 \partial x_a^4 \partial (y_a - h_0)}\right) \tag{32}$$

$$g_{i/222} = \frac{1}{8}\left(\frac{\partial^6 V_i}{\partial x_a^2 \partial (y_a - h_0)^4} - 2\frac{\partial^6 V_i}{\partial h_0 \partial x_a^2 \partial (y_a - h_0)^3} + \frac{\partial^6 V_i}{\partial h_0^2 \partial x_a^2 \partial (y_a - h_0)^2}\right) \tag{33}$$

$$g_{i/204} = \frac{1}{48}\left(\frac{\partial^6 V_i}{\partial (y_a - h_0)^6} - 2\frac{\partial^6 V_i}{\partial h_0 \partial (y_a - h_0)^5} + \frac{\partial^6 V_i}{\partial h_0^2 \partial (y_a - h_0)^4}\right) \tag{34}$$

$$g_{i/141} = \frac{1}{24}\left(-\frac{\partial^6 V_i}{\partial x_a^4 \partial (y_a - h_0)^2} + \frac{\partial^6 V_i}{\partial h_0 \partial x_a^4 \partial (y_a - h_0)}\right) \tag{35}$$

$$g_{i/123} = \frac{1}{12}\left(-\frac{\partial^6 V_i}{\partial x_a^2 \partial (y_a - h_0)^4} + \frac{\partial^6 V_i}{\partial h_0 \partial x_a^2 \partial (y_a - h_0)^3}\right) \tag{36}$$

$$g_{i/105} = \frac{1}{120}\left(-\frac{\partial^6 V_i}{\partial (y_a - h_0)^6} + \frac{\partial^6 V_i}{\partial h_0 \partial (y_a - h_0)^5}\right) \tag{37}$$

$$g_{i/042} = \frac{1}{48}\left(\frac{\partial^6 V_i}{\partial x_a^4 \partial (y_a - h_0)^2}\right) \tag{38}$$

$$g_{i/024} = \frac{1}{48}\left(\frac{\partial^6 V_i}{\partial x_a^2 \partial (y_a - h_0)^4}\right) \tag{39}$$

$$g_{i/060} = \frac{1}{720}\left(\frac{\partial^6 V_i}{\partial x_a^6}\right) \tag{40}$$

$$g_{i/006} = \frac{1}{720}\left(\frac{\partial^6 V_i}{\partial (y_a - h_0)^6}\right) \tag{41}$$

References

[1] W. J. Smith, *Modern Optical Engineering,* 3rd ed., (Edmund Industrial Optics, Barrington, N. J., (2001), p. 62.

[2] W. T. Welford*, Aberrations of Optical Systems* (Adam Hilger, 1986).

[3] V. N. Mahajan, *Optical Imaging and Aberrations*, Part I Ray Geometrical Optics (SPIE Press, 1998).

[4] R. Kingslake and R. B. Johnson, *Lens Design Fundamentals, Second Edition* (Academic, 2010).

[5] J. Sasián, *Introduction to Aberrations in Optical Imaging Systems* (Cambridge, 2013).

[6] H. A. Buchdahl, *Optical Aberration Coefficients* (Dover, 1968).

[7] G. W. Hopkins, "Proximate ray tracing and optical aberration coefficients," J. Opt. Soc. Am. 66 (5), 405–410 (1976).

[8] W. T. Welford, "A new total aberration formula," J. Mod. Opt. 19, 719–727 (1972).

[9] B. Chen and A. M. Herkommer, "High order surface aberrations contributions from phase space analysis of differential rays," Opt. Express 24, 5934–5945 (2016).

[10] D. Claus, J. Watson, and J. Rodenburg, "Analysis and interpretation of the Seidel aberration coefficients in digital holography," Appl. Opt. 50 (34), H220–H229 (2011).

[11] R. S. Chang, J. Y. Sheu, and C. H. Lin, "Analysis of Seidel aberration by use of the discrete wavelet transform," Appl. Opt. 41 (13), 2408–2413 (2002).

[12] R. B. Johnson, "Polynomial ray aberrations computed in various lens design programs," Appl. Opt. 12 (9), 2079–2082 (1973).

[13] M. Oleszko, R. Hambach, and H. Gros, "Decomposition of the total wave aberration in generalized optical systems," J. Opt. Soc. Am. 34 (10), 1856–1864 (2017).

[14] R. B. Johnson, "Balancing the astigmatic fields when all other aberrations are absent," Applied Optics 32 (19), 3494–3496 (1993).

[15] P. D. Lin and R. B. Johnson, "Seidel Aberration Coefficients: an Alternative Computation Method," Opt. Express 27 (14), 19712–19725 (2019).

[16] P. D. Lin, " Seidel primary ray aberration coefficients for objects placed at finite and infinite distances," Opt. Express 28 (9), 19740–19754 (2020).

[17] P. D. Lin, "Alternative method for computing primary wavefront aberrations using Taylor series expansion of optical path length", OPTIK - International Journal for Light and Electron Optics, Vol. 248, Article 168134, November 2021.

[18] "Zemax OpticStudio 18.9 User Manual," (Zemax LLC, 2018).

[19] S. Jibrin and I. Abdullahi, "Search directions in infeasible newton's method for computing weighted analytic center for linear matrix inequalities," Applied and Computational Mathematics. *8* (1), 21–28 (2019).

[20] BA Demba Bocar, "Uniform convergence of the series expansion of the multifractional brownian motion," Applied and Computational Mathematics. *9* (6), 195–200 (2020).

[21] M. M. Aliyev, "Exact, polynomial, determination solution method of the subset sum problem," Applied and Computational Mathematics. *3* (5), 262-267 (2014).